

An evaluation of constitutive models to predict the behaviour of fine-grained soils with different degrees of overconsolidation

V. Hájek & D. Mašín
Charles University, Prague

ABSTRACT: Incorporation of void ratio as a state variable into constitutive models allows, in principle, to use a single set of material parameters for soils with different degrees of overconsolidation. p constant experiments by Hattab and Hicher (2004) on soils with overconsolidation ratios (OCR) ranging from 1 to 50 are used for evaluation of three constitutive models of different complexity. It is demonstrated by means of a scalar error measure and stress-strain diagrams that at least two sets of parameters for different OCR intervals should be used. Further, advanced models perform significantly better than the Modified Cam clay model and a hypoplastic model for clays leads to better predictions than elasto-plastic three surface kinematic hardening model.

1 INTRODUCTION

It has been recognised since the development of critical state soil mechanics in 1960's that realistic constitutive models should consider void ratio e as a state variable. This approach, in theory, allows to use a single set of material parameters to predict the behaviour of soils with a broad range of overconsolidation ratios and thus simplifies practical application of constitutive models. As a matter of fact, however, qualitatively correct predictions of behaviour of soils with different OCR s based on a single set of material parameters do not necessarily imply satisfactory performance from the quantitative point of view. An engineer aiming to apply the constitutive model for solution of practical geotechnical problems should be aware of the range of OCR s for which a single set of material parameters may be used and design an experimental program accordingly.

In the present paper, performance of three constitutive models of different complexity is evaluated on the basis of triaxial tests by Hattab and Hicher (2004). Reconstituted kaolin clay was isotropically consolidated up to $p_{max} = 1000$ kPa and swelled to a mean effective stress $p = p_{max}/OCR$, with overconsolidation ratios ranging from 1 to 50. From this state a shear phase with constant mean stress p followed up to failure.

2 CONSTITUTIVE MODELS

Modified Cam clay model (CC) has been chosen as a reference for comparison with two advanced consti-

tutive models based on different mathematical backgrounds, namely the three surface kinematic hardening model (3SKH), and a hypoplastic model for clays (HC).

Modified Cam clay model (Roscoe and Burland 1968) is a basic critical state soil mechanics model. In this work a version which complies with Butterfield's (1979) compression law is used, thus the isotropic virgin compression line reads

$$\ln(1 + e) = N - \lambda^* \ln(p/p_r) \quad (1)$$

with parameters N and λ^* and a reference stress $p_r = 1$ kPa. Slope of the isotropic unloading line is controlled by the parameter κ^* , constant shear modulus G is assumed inside the yield surface and the critical state stress ratio is characterised by parameter M .

The 3SKH model (Stallebrass and Taylor 1997) is an advanced example of the kinematic hardening plasticity models for soils. The model, which may be seen as an evolution of the CC model, is characterised by two kinematic surfaces in the stress space (see Fig. 1), which determine the extent of the elastic behaviour (yield surface) and the influence of the recent stress history (history surface).

Parameters N , λ^* , κ^* and M have the same meaning as in the CC model, the shear modulus inside the elastic range G is calculated from

$$\frac{G}{p_r} = A \left(\frac{p}{p_r} \right)^n OCR^m \quad (2)$$

with parameters A , n and m . Parameters T and S characterise relative sizes of kinematic surfaces

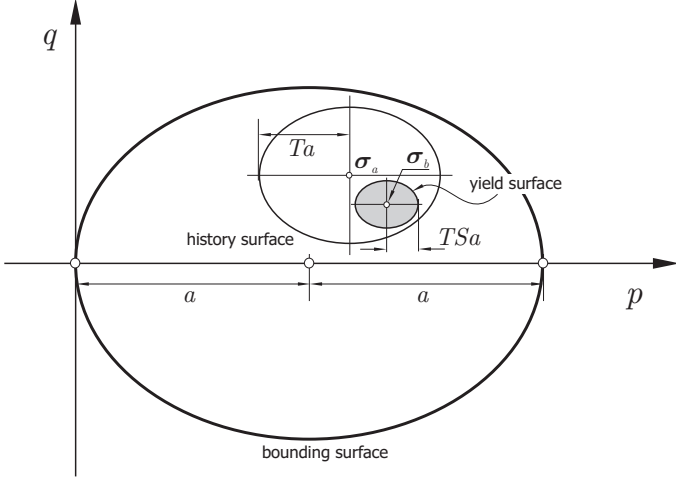


Figure 1. Characteristic surfaces of the 3-SKH model, from Mašín et al., 2006.

(Fig. 1). The last parameter ψ controls the rate of decay of both bulk and shear moduli for states at the yield surface, inside bounding surface (Fig. 1).

A hypoplastic constitutive model for clays was proposed by Mašín (2005) and investigated further by Mašín and Herle (2005). It combines the mathematical formulation of hypoplastic models (e.g., Kolymbas 1991) with the basic principles of the CC model. The rate formulation is governed by a single non-linear equation

$$\dot{\boldsymbol{\sigma}} = f_s \mathcal{L} : \dot{\boldsymbol{\epsilon}} + f_s f_d \mathbf{N} \|\dot{\boldsymbol{\epsilon}}\| \quad (3)$$

with constitutive tensors \mathcal{L} and \mathbf{N} and scalar factors f_s and f_d , no switch function is introduced to distinguish between loading and unloading and strains are not sub-divided into elastic and plastic parts as in elasto-plasticity.

The model requires five parameters with a similar physical interpretation as parameters of the CC model. N and λ^* are coefficients in the Butterfield's (1979) compression law (1), κ^* controls the slope of the isotropic unloading line in the $\ln(1+e)$ vs. $\ln(p/p_r)$ space, φ_c is the critical state friction angle. The last parameter r determines the shear modulus. Due to non-linear character of Eq. (3), the parameter r is usually calibrated by means of a parametric study, similarly to the parameter ψ of the 3SKH model.

3 SCALAR ERROR MEASURE

A scalar error measure has been introduced in order to assess model performance in the pre-failure regime and in order to eliminate a high amount of subjectivity of model calibration.

The suitable error measure should reflect differences in both predicted and observed stiffnesses and strain path directions. As experiments and simulations are characterised by identical stress paths, simulation error is measured in the strain space. Let the pre-failure part of the stress path be subdivided into L

increments, of length $\Delta q = q_{max}/L$. Then, following Mašín et al. (2006), the simulation error can be defined as

$$err(OCR, q_{max}) = \frac{\sum_{k=1}^L \|\Delta \boldsymbol{\epsilon}_{sim}^{(k)} - \Delta \boldsymbol{\epsilon}_{exp}^{(k)}\|}{\sum_{k=1}^L \|\Delta \boldsymbol{\epsilon}_{exp}^{(k)}\|} \quad (4)$$

where $\Delta \boldsymbol{\epsilon}_{exp}^{(k)}$ and $\Delta \boldsymbol{\epsilon}_{sim}^{(k)}$ are the measured and predicted strain increment tensors, respectively, corresponding to the k -th stress increment of size Δq .

In order to demonstrate the meaning of the numerical value of err , it is plotted for two special cases in Fig. 2. First, experiment and simulation with identical strain path directions and different incremental stiffnesses (measured by their ratio $\alpha = \|\Delta \boldsymbol{\epsilon}_{exp}^{(k)}\| / \|\Delta \boldsymbol{\epsilon}_{sim}^{(k)}\|$ from (4), i.e. $\alpha = G_{sim}/G_{exp} = K_{sim}/K_{exp}$, where G and K are shear and bulk moduli respectively) are considered. In the second case experiment and simulation are characterised by identical incremental stiffnesses ($\alpha = 1$), but different directions of the strain paths measured by the angle ψ_ϵ in the Rendulic plane of $\boldsymbol{\epsilon}$ (ϵ_a vs. $\sqrt{2}\epsilon_r$, where ϵ_a and ϵ_r are axial and radial strains respectively). Investigation of (4) reveals that $err = |1 - 1/\alpha|$ for the first case and $err = |2 \sin(\Delta\psi_\epsilon/2)|$ for the second one (with $\Delta\psi_\epsilon = \psi_{\epsilon sim} - \psi_{\epsilon exp}$).

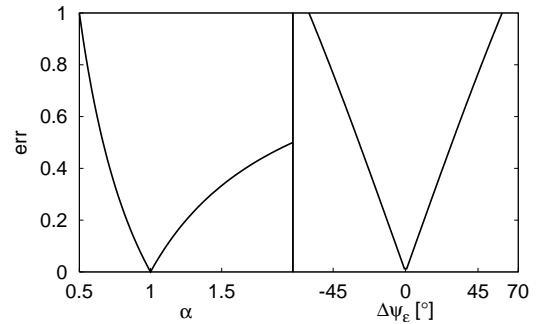


Figure 2. Numerical values of err for experiments and simulations that differ only in incremental stiffnesses (left) and strain path directions (right).

Calculation of err is complicated by the scatter in experimental data, in particular for low p (high OCR). For calculating of err the data were approximated by polynomial functions of the form

$$\epsilon_s = a_s q^{b_s} + c_s q^{d_s} + e_s q^{f_s} \dots \quad (5)$$

and

$$\epsilon_v = a_v q^{b_v} + c_v q^{d_v} + e_v q^{f_v} \dots \quad (6)$$

with coefficients $a_s, b_s, c_s, d_s, e_s, f_s \dots$ and $a_v, b_v, c_v, d_v, e_v, f_v \dots$. In this way a good fit of experimental data was achieved, as demonstrated in Fig. 3 for an experiment with $OCR = 10$.

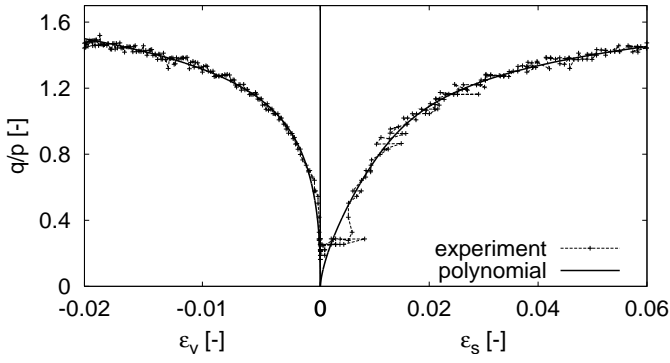


Figure 3. Approximation of experimental data for $OCR = 10$ by a polynomial function.

In the present work, for all simulations q_{max} from (4) is chosen such that $q_{max} = 0.7q_{peak}$, where q_{peak} is the peak deviator stress achieved in the particular experiment. L in (4) is high enough so it does not influence calculated err (typically $L = 100$ was used).

4 CALIBRATION

The parameters of the studied constitutive models can be roughly split into two groups. In one group are parameters with a clear physical meaning, which are calibrated by standardized calibration procedures. On the other hand, parameters from the second group are less clearly defined and their calibration is more subjective. These parameters are usually found by means of parametric studies.

4.1 The first group of parameters

In the present work, parameters from the first group were calibrated only once and their values were kept constant for all simulations.

To this group belong parameters N , λ^* and κ^* , which were found by evaluation of an isotropic loading and unloading test, as demonstrated for the CC model in Fig. 4. Note that the numerical values of the parameter κ^* (Tab. 1) differ for the three constitutive models. In the 3SKH model κ^* specifies a bulk stiffness in the *small strain* range and it was calculated from an assumed Poisson ratio (accurate volumetric measurements in the small strain range were not available). In the HC model the slope of the isotropic unloading line is for higher $OCRs$ influenced also by the non-linear character of the hypoplastic equation. For this reason κ^* of the HC model could be considered to belong to the second group of parameters. However, as it has only minor effect on predictions of constant p experiments (which are in scope of this study), its value was kept constant for all simulations. An approximate average value of the critical state friction angle from all shear experiments available was used to calculate the parameter M (φ_c).

The 3SKH model requires five further parameters that control the behaviour in the small strain range

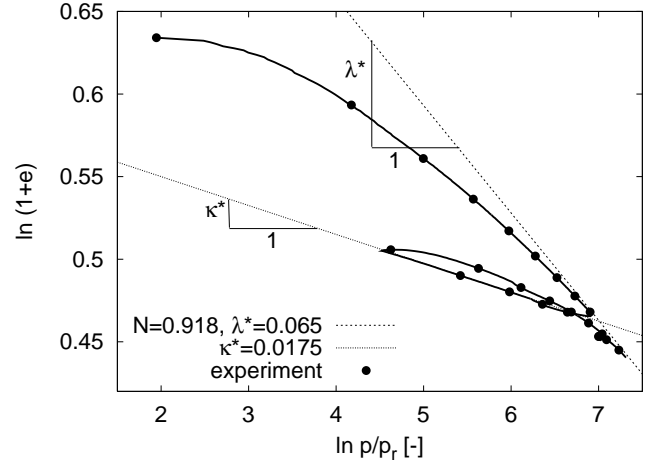


Figure 4. Calibration of parameters N , λ^* and κ^* of the CC model.

and the influence of the recent history (A , n , m , T and S). Data by Hattab and Hicher (2004) do not contain experiments required for their calibration. However, as similar soil (Speswhite kaolin) was used by Stallebrass and Taylor (1997), the additional parameters of the 3SKH model were taken over from their work.

4.2 The second group of parameters

These parameters, namely G (CC), r (HC) and ψ (3SKH), influence significantly results of constant p experiments in the pre-failure regime and their calibration is to some extent subjective. In order to eliminate this subjectivity, these parameters were found by minimizing the scalar error measure err defined in Sec. 3. This procedure was applied on constant p experiments at $OCR = 1$ and $OCR = 10$, so two sets of material parameters (optimised for $OCR = 1$ and $OCR = 10$) were obtained (Tab. 1).

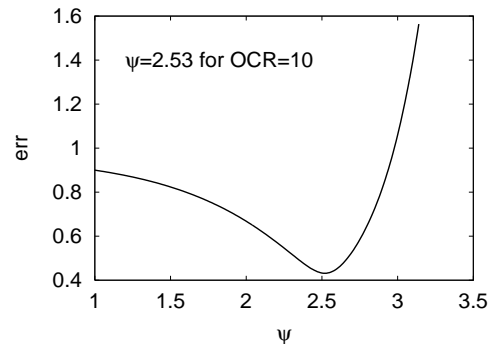


Figure 5. Calibration of ψ by means of minimalisation of err for experiment at $OCR = 10$.

Calibration of parameters from the second group is in the following demonstrated by means of calibration of ψ using an experiment at $OCR = 10$.

Relation of err with respect to the value of ψ is shown in Fig. 5. The curve has a clear minimum that corresponds to $\psi = 2.53$. This optimised value of ψ , together with two different values, were used for simulation of the experiment at $OCR = 10$ (Fig. 6). In

the pre-failure regime the value of ψ found by optimisation with respect to err corresponds quite well to the value that could have been chosen by means of a subjective trial-and-error calibration procedure.

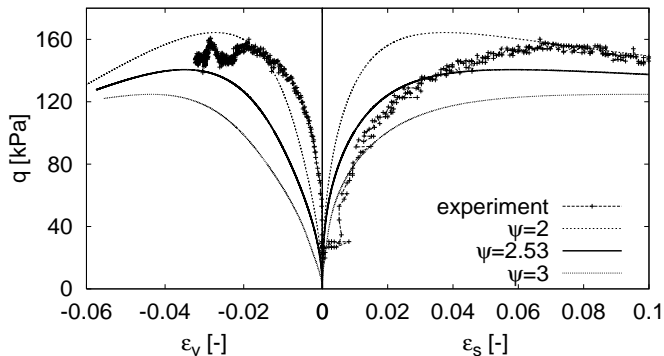


Figure 6. Predictions of the test OCR=10 by the 3SKH model with err -optimised ($\psi = 2.53$) and two different values of ψ .

Parameters r and G were found using the same procedure as outlined above, a clear minimum of err was obtained in all cases. The only difference was in the calibration of ψ for $OCR = 1$, as the stress state of the 3SKH model is on the bounding surface and therefore ψ does not influence model predictions. In this case ψ was found by trial-and-error by simulation of the isotropic unloading test from Fig. 4.

Table 1. Material parameters

	M, φ_c	λ^*	κ^*	N		
CC	1.1	0.065	0.0175	0.918		
HC	27.5°	0.065	0.01	0.918		
3SKH	1.1	0.065	0.0034	0.918		
	A	n	m	T	S	
3SKH	1964	0.65	0.2	0.25	0.08	
	G, r, ψ (OCR1)		G, r, ψ (OCR10)			
CC	7330 kPa		2210 kPa			
HC	1.43		0.67			
3SKH	2.3		2.53			

5 PERFORMANCE OF THE MODELS

The two sets of parameters found in Sec. 4 were used in simulating experiments at the whole range of $OCRs$. The initial states of p' , q and e measured in the experiments were used in the simulations. In addition, the 3SKH model requires to specify the initial positions of kinematic surfaces. These were aligned to reflect the stress history followed in the experiments (Sec. 1).

The obtained scalar error measure err is plotted with respect to OCR in Fig. 7. From this figure it appears that studied elasto-plastic and hypoplastic mod-

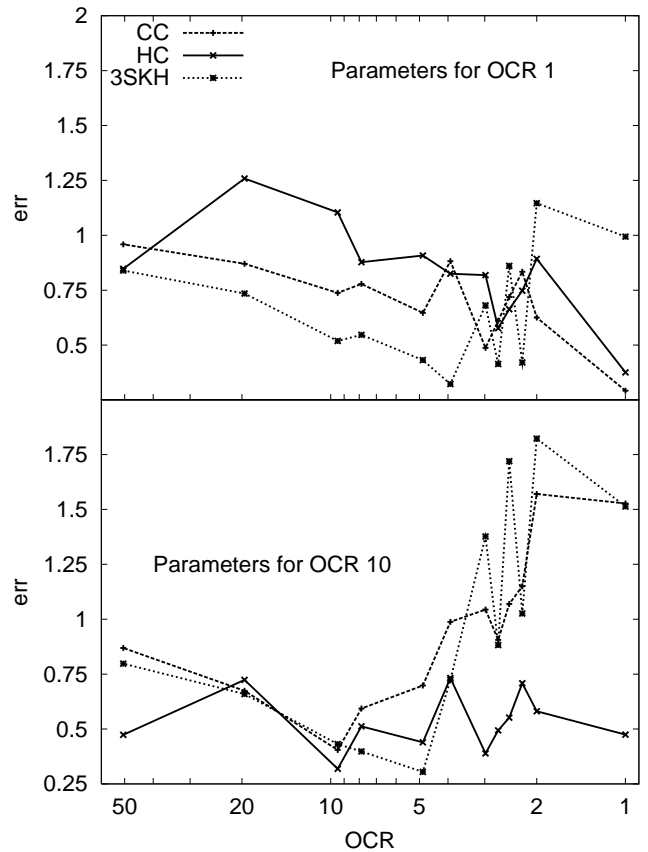


Figure 7. err for parameters optimised for $OCR = 1$ (top) and $OCR = 10$ (bottom).

els have different ranges of validity of different sets of material parameters:

1. Hypoplastic (HC) model performs for higher $OCRs$ less correctly than other two models when calibrated using data for $OCR = 1$. However, when calibrated at higher OCR , it produces the best predictions out of all tested models for the entire range of $OCRs$, with more-or-less constant value of err .
2. Elasto-plastic (CC and 3SKH) models calibrated at $OCR = 10$ perform relatively correctly up to $OCR \approx 4$. For lower $OCRs$ parameters for normally consolidated state lead to better predictions, but in the case of 3SKH still worst than predictions by hypoplasticity.

By definition, the value of err characterises model predictions in the pre-failure regime only. In order to evaluate predictions at failure, observed and predicted peak friction angles φ_p were plotted with respect to OCR . The results were similar for both sets of parameters, Fig. 8 shows them for parameters optimised for $OCR = 10$. HC and 3SKH models predict peak friction angles relatively accurately (HC is more accurate for $OCR \leq 10$, 3SKH for $OCR \geq 20$). CC model overestimates significantly φ_p for all states with $OCR > 2$. This is a well-known shortcoming of

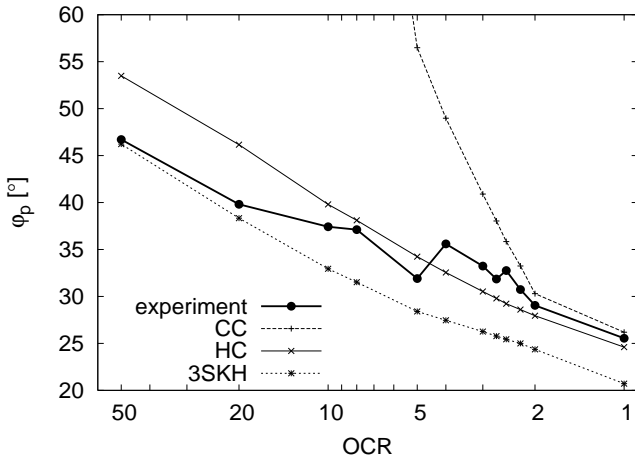


Figure 8. Peak friction angles φ_p predicted by the models with parameters optimised for $OCR = 10$.

the CC model, caused by the elliptical shape of the yield surface.

While err gives a convenient quantitative measure of the model performance, it does not specify the source of the prediction error. For qualitative comparison, the stress paths normalised by the Hvorslev equivalent pressure p_e^* are plotted for $OCR = 10$ optimised parameters in Fig. 9. Overprediction of φ_p by the CC model is clear, the shape of the normalised stress paths is predicted relatively correctly by both HC and 3SKH models. All models, however, overestimate dilation. Normalised stress paths of all models head towards a unique critical state point, which has not been reached in the experiments at higher $OCRs$ (Fig. 9 top). A possible reason may be in localisation of deformation in shear bands at higher $OCRs$.

q vs. ϵ_s graphs for $OCR = 10$ optimised parameters are shown in Fig. 10. It is clear that higher errors for low $OCRs$ of elasto-plastic models, reflected in Fig. 7, are caused by the underestimation of the shear stiffness in the case of CC and overestimation of the shear stiffness in the case of 3SKH (with the exception of $OCR = 1$). Low prediction errors by the HC model (Fig. 7) are reflected also in qualitatively correct performance shown in Fig. 10. Volumetric changes shown in Fig. 11 reveal a general trend of overestimation of dilation for higher $OCRs$, as already discussed in the previous paragraph. The shape of ϵ_v vs. ϵ_s curves is best predicted by the HC model. For high $OCRs$ the 3SKH model predicts dilatant behaviour immediately after the start of the shear phase, which has not been observed in the experiments. On the other hand, hypoplasticity overestimates the initial contraction for medium $OCRs$.

6 CONCLUDING REMARKS

Results of this study must be seen as preliminary, as only one set of experimental data on one particular soil was investigated. Presented results however show that at least two sets of material parameters should

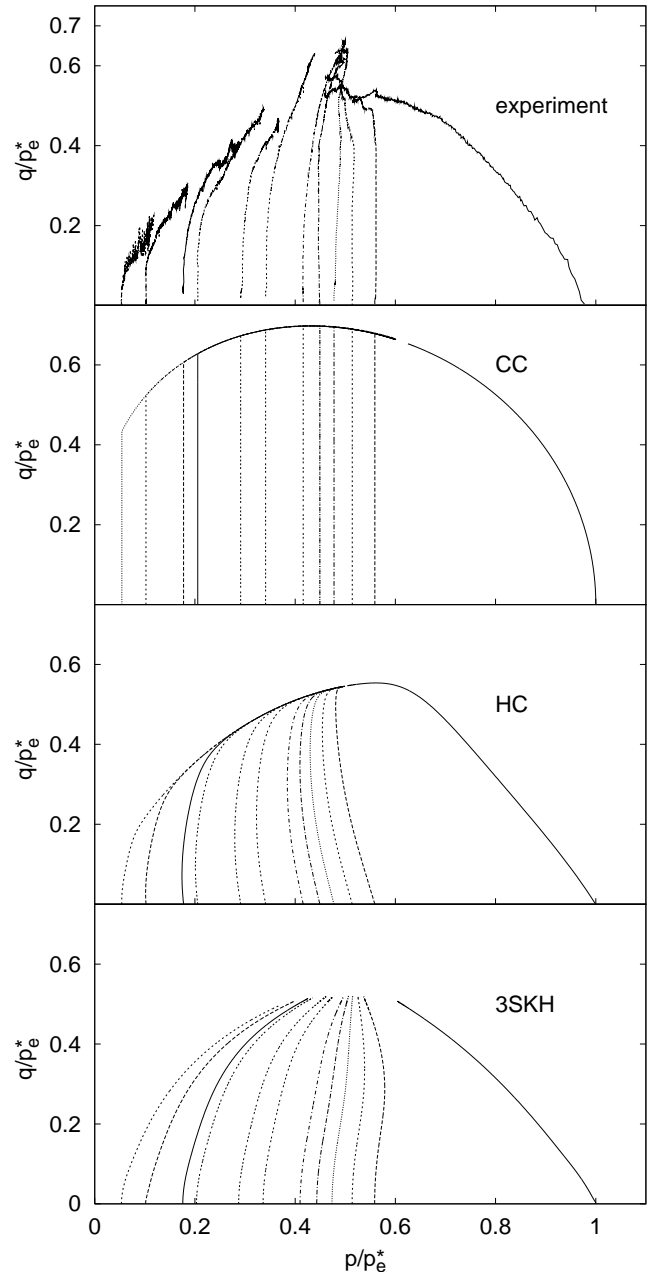


Figure 9. Stress paths normalised by p_e^* for $OCR = 10$ optimised parameters.

be considered for both hypoplastic and elasto-plastic models. It appears that the HC model requires a different set of material parameters only for normally consolidated soil, a single set of parameters, which leads to accurate predictions for a broad range of $OCRs$, is sufficient for $OCR > 1$. Two sets of parameters should also be used for studied elasto-plastic models, with the approximate limiting $OCR \approx 4$.

It is perhaps not surprising that the two advanced models performed significantly better than the CC model in predicting the non-linear behaviour in the pre-failure regime and correctly estimating the peak friction angles for high $OCRs$. For higher $OCRs$ the HC model leads to better predictions than the 3SKH, both from the point of view of the scalar error measure err and a qualitative performance expressed by

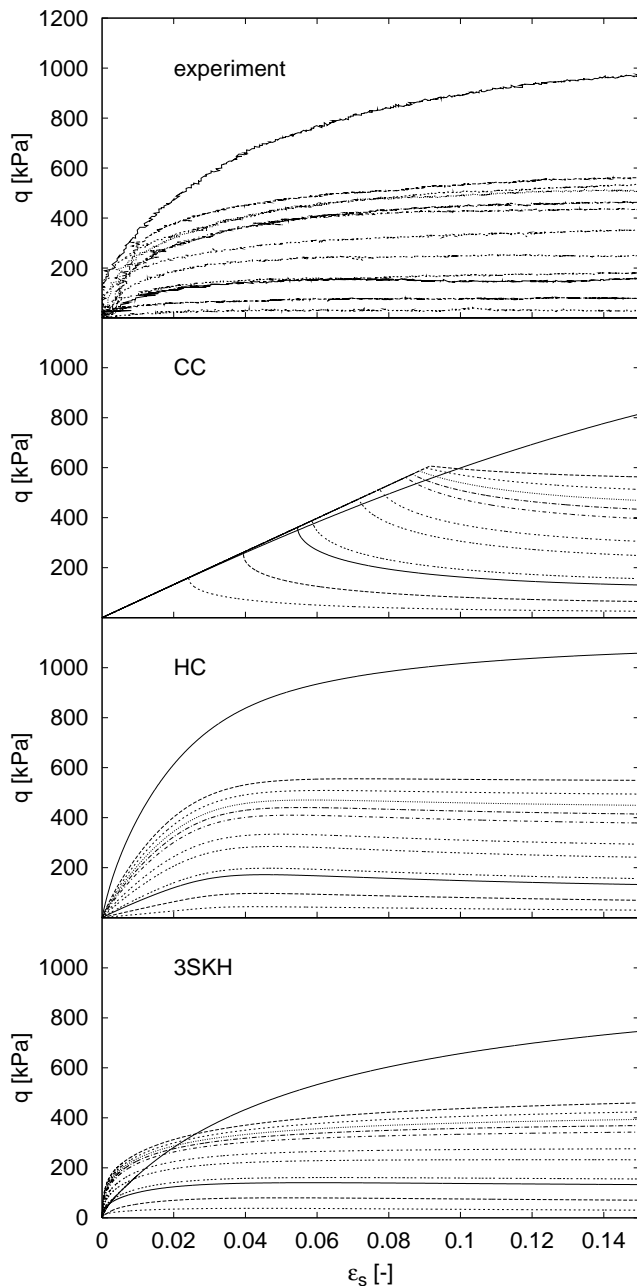


Figure 10. q vs. ϵ_s graphs for $OCR = 10$ optimised parameters.

the stress - strain diagrams. Also, the 3SKH model can not be effectively calibrated to predict correctly the behaviour of soils in normally consolidated state.

7 ACKNOWLEDGEMENT

Experimental data on kaolin clay were kindly provided by Prof. Mahdia Hattab. Financial support by the research grant GAAV IAA200710605 is gratefully acknowledged.

REFERENCES

- Butterfield, R. (1979). A natural compression law for soils. *Géotechnique* 29(4), 469–480.
- Hattab, M. and P.-Y. Hicher (2004). Dilating behaviour of overconsolidated clay. *Soils and Foundations* 44(4), 27–40.
- Kolymbas, D. (1991). An outline of hypoplasticity. *Archive*

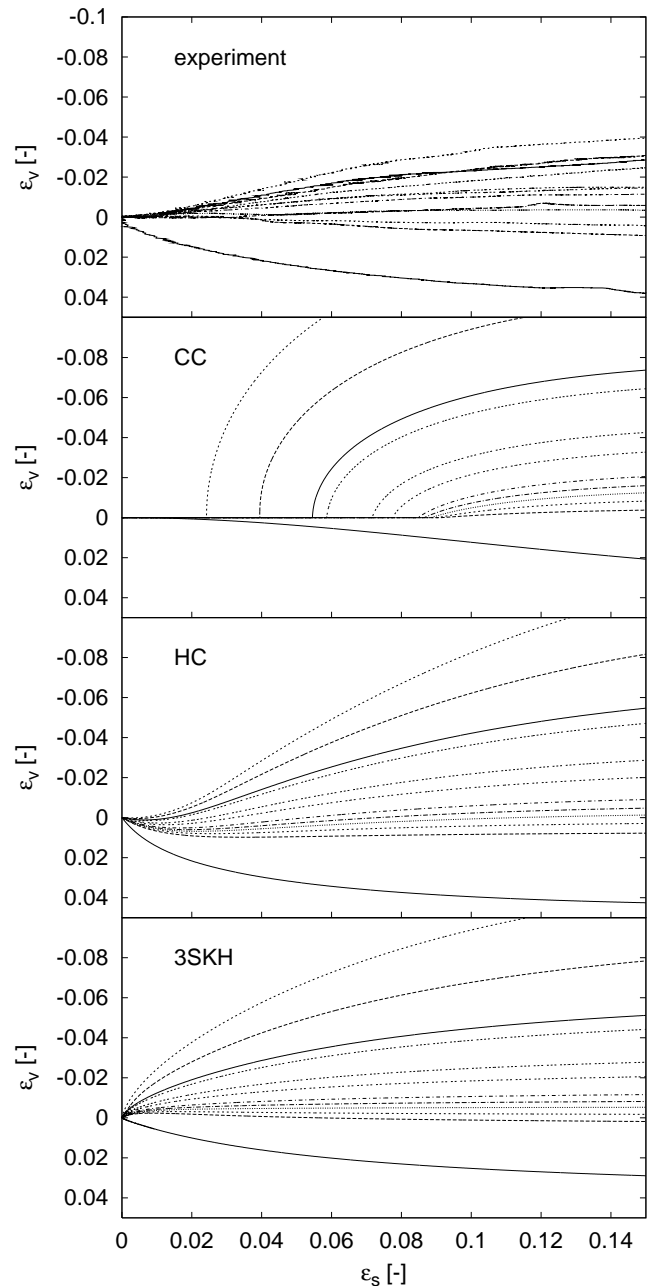


Figure 11. ϵ_v vs. ϵ_s graphs for $OCR = 10$ optimised parameters.

of Applied Mechanics 61, 143–151.

- Mašín, D. (2005). A hypoplastic constitutive model for clays. *International Journal for Numerical and Analytical Methods in Geomechanics* 29(4), 311–336.
- Mašín, D. and I. Herle (2005). State boundary surface of a hypoplastic model for clays. *Computers and Geotechnics* 32(6), 400–410.
- Mašín, D., C. Tamagnini, G. Viggiani, and D. Costanzo (2006). Directional response of a reconstituted fine grained soil. Part II: Performance of different constitutive models. *International Journal for Numerical and Analytical Methods in Geomechanics* (reviewed).
- Roscoe, K. H. and J. B. Burland (1968). On the generalised stress-strain behaviour of wet clay. In J. Heyman and F. A. Leckie (Eds.), *Engineering Plasticity*, pp. 535–609. Cambridge: Cambridge University Press.
- Stallebrass, S. E. and R. N. Taylor (1997). Prediction of ground movements in overconsolidated clay. *Géotechnique* 47(2), 235–253.